Macromolecules

pubs.acs.org/Macromolecules Article

Impact of Reversible Deactivation Radical Copolymerizations (RDRPs) on Gelation, Phase Separation, and Mechanical Properties of Polymer Networks

Aaliyah Z. Dookhith, Zidan Zhang, Venkat Ganesan, and Gabriel E. Sanoja*

Cite This: Macromolecules 2024, 57, 8698–8711 Read Online

ACCESS | Metrics & More | Article Recommendations | Supporting Information

ABSTRACT: Polymer networks are widely used in engineering and biomedical applications because they can sustain large deformations. However, their mechanical properties, particularly at large strains, remain challenging to design within their molecular architecture through conventional synthetic methods, as these offer limited control over the kinetics and thermodynamics of gelation and, in turn, the connectivity of the polymers. In this work, we leverage recent advances in Reversible Deactivation Radical Copolymerizations (RDRPs) to tune the kinetics and thermodynamics of gelation and explore their impact on the molecular architecture and mechanical properties of polymer networks. We demonstrate that RDRPs lead to delayed gelation, phase separation, and softer and more extensible networks relative to conventional free radical copolymerizations. The reversible deactivation of the radical chain ends slows the kinetics of gelation, segregates the network precursors or clusters into cross-linker-rich and cross-linker-poor phases, and narrows the distribution of chain lengths within the polymers. This impact of the kinetics of gelation on the molecular architecture affects the load distribution among the constituent polymers and the interplay between the small- and large-strain mechanical properties. Overall, this work paves the way for rationally using polymer chemistry to design advanced polymer networks for emerging and more stringent applications.

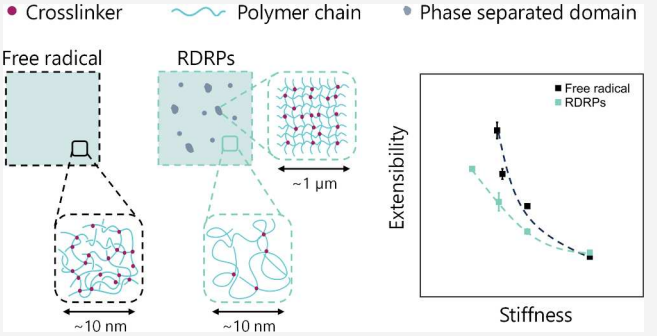

INTRODUCTION

Polymer networks date back to the 15th century when Amazon Indian civilizations reacted latex from rubber trees with oxygen from air to form elastic, brittle, and unstable rubbers. Since then, Charles Goodyear vulcanized natural rubber, researchers at I.G. Farben introduced synthetic Styrene−Butadiene−Rubber (SBR), and the rubber industry developed materials that today are widespread in our daily lives, such as elastomers in rubber tires, dampers, and seals, pressure-sensitive adhesives (PSAs) in tapes, and hydrogels in contact lenses and superabsorbent diapers.[1−3] Despite such progress, it remains challenging to rationally design the network architecture and mechanical properties through conventional synthetic methods, particularly at large strains where the polymer chains elongate far from their Gaussian configuration and close to their contour length.

The reasons for such a challenge are 2-fold. First, polymer networks form by gelation, a process in which polymer melts, concentrated solutions, or monomer-cross-linker mixtures react to form a three-dimensional structure comprised of a broad distribution of elastically active chains and topological defects such as loops and dangling chains.[4] This distribution governs the elongation and load carried by the individual polymers, and the nucleation and growth of microscopic cracks. However, characterizing this distribution experimentally is challenging, and, to our knowledge, only possible in a subset of poly(ethylene glycol) networks cross-linked through click chemistry.[5−9] Second, polymer networks can undergo phase separation during gelation and arrest concentration fluctuations within their architecture.[10,11] These fluctuations have different densities of elastically active chains and unevenly distribute the load among the polymer chains. Notably, the rate of gelation plays a key role in the phase behavior of polymer networks but cannot be controlled with conventional synthetic methods such as chain- and step-growth polymerizations. Controlling such a rate with new synthetic methods could serve to understand the relationship between network synthesis, architecture, and small- and large-strain mechanical properties.

To this end, numerous investigations have focused on tailoring the architecture and mechanical properties of polymer

Received: April 20, 2024
Revised: July 8, 2024
Accepted: August 30, 2024
Published: September 10, 2024

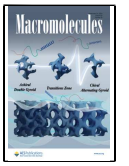

https://doi.org/10.1021/acs.macromol.4c00905
Macromolecules 2024, 57, 8698−8711

networks by end-linking low-molecular-weight oligomers in bulk or concentrated solutions, such as poly(ethylene glycol),[5,12,13] poly(propylene glycol),[14,15] and poly(dimethylsiloxane) chains.[16] Using this strategy, Cohen and co-workers unveiled the effect of oligomer concentration and molecular weight on the cross-link and entanglement densities, elasticity, and strain softening of poly(dimethylsiloxane) networks.[17,18] In more recent studies, Olsen, Zhao, Crosby, Peppas, and co-workers similarly controlled the molecular connectivity of poly(ethylene glycol) networks and investigated the impact of topological defects on their bulk elasticity, swelling, diffusion, and fracture toughness.[5,7,8,13,19−22] These studies refined longstanding molecular models such as rubber elasticity, Flory−Rehner, and Lake−Thomas,[23−25] and provided guidelines to design polymer networks with advanced physical properties.

More elusive structure−property relationships exist in polymer networks synthesized by chain growth copolymerization of monomer and cross-linker, such as the poly(hydroxyethyl methacrylamide) hydrogels used in soft contact lenses and the poly(ethyl acrylate) elastomers used in O-rings, gaskets, or seals. Typically, these copolymerizations are uncontrolled and involve the rapid reaction of monomers and cross-linkers to form covalent bonds and reactive chain ends. Termination events lead to "dead" gels or clusters at low conversion and a polymer network at the gel point.[26−28] However, excluded volume interactions can lead to polymer-rich and polymer-poor phases at high conversions (i.e., microsyneresis), which impact the bulk properties of the networks. Specifically, phase-separated networks are more opaque, swellable, and softer than their macroscopically "homogeneous" analogues.[29−38]

Over the past decades, reversible deactivation radical polymerizations (RDRPs) have emerged as techniques to control the synthesis of linear polymers.[39] These techniques include reversible addition−fragmentation chain transfer (RAFT), atom transfer radical polymerization (ATRP), and nitroxide-mediated polymerization (NMP), and lead to polymers of narrow dispersity and well-defined molecular weight. However, RDRPs remain relatively unexplored for synthesizing polymer networks. Fukuda, Billingham and Armes, Matyjaszewski, and co-workers have argued that these techniques prevent the formation of "dead" gels or clusters at low conversions and, as a result, enable a more homogeneous distribution of "dormant" gels or branched polymers that percolate into a network at higher conversions or percolation thresholds.[40−49] Yet, this picture raises several issues that remain unresolved, including (i) the impact of the kinetics of copolymerization on the distribution of elastically active chains, loops, and dangling chains; (ii) the effect of delayed gelation on phase separation; and (iii) the influence of RDRPs on the small- and large-strain mechanical properties of polymer networks.

This work addresses the above issues by considering a series of polymer networks synthesized by free radical, RAFT, and ATRP copolymerization of an ethyl acrylate monomer and a 1,4-butanediol diacrylate cross-linker. The copolymerizations are conducted in bulk or concentrated solution (90% v/v), the percolation thresholds are estimated from the vinyl conversion at which the monomer-cross-linker mixture undergoes gelation, and phase separation is examined by optical microscopy and light transmittance. The mechanical properties are probed experimentally by linear amplitude oscillatory shear rheology and uniaxial tensile tests, interpenetrating the networks within a soft and extensible matrix (i.e., within a multiple-network architecture) to evaluate the limiting extensibility of the polymer chains. The copolymerizations are complemented by reactive Monte Carlo simulations, which are used to characterize the distributions of elastically active chains and topological defects within the networks. The key result of our work is that RDRPs lead to higher percolation thresholds, phase separation, and softer and less extensible networks. The reversible deactivation of the propagating radicals impacts the competition between gelation and phase separation and the distribution of elastically active chains. Overall, this result paves the way for synthesizing polymer networks with advanced mechanical properties, accelerating the development of emerging technologies like additive manufacturing, artificial tissue scaffolds, and soft robotics.

MATERIALS AND METHODSS

Materials. Unless otherwise specified, all chemicals were used as received. Ethyl acrylate (EA) and 1,4-butanediol diacrylate (BDA) were sourced from TCI; 2-hydroxy-2-methylpropiophenone (HMP), cyanomethyl dodecyl trithiocarbonate (CTA), ethyl α-bromoisobutyrate (EBiB), copper(I) bromide (CuBr), tris[2-(dimethylamino)-ethyl]amine (Me_6TREN), and anhydrous ethyl acetate from Millipore Sigma; basic aluminum oxide, toluene, anhydrous dimethyl sulfoxide (DMSO) and HPLC grade chloroform from VWR; and deuterated chloroform from Cambridge Isotopes.

EA (100 mL) and BDA (25 mL) were purified by elution over basic aluminum oxide. Purified EA, BDA, and as-received HMP, EBiB, and Me_6TREN were placed in dry septum-sealed bottles, sparged with N_2 for 45 min, and transferred into a N_2-filled glovebox.

Polymerization of Ethyl Acrylate (EA): Linear polymers. Linear polymers were synthesized in a N_2-filled glovebox, targeting a molecular weight of 100 kDa. Depending on the polymerization mechanism, the concentration of the initiator (free radical and ATRP) or the chain transfer agent (RAFT) was fixed at ∼0.1 mol % to control the concentration of the propagating radicals (i.e., chain ends). However, the control of this concentration was poor in the free radical polymerization due to an excessive number of termination events in the absence of a reversible deactivation step.

For free radical polymerizations, monomer EA and initiator HMP (0.1 mol %) were mixed in a 20 mL scintillation vial and transferred to a mold composed of two polyethylene terephthalate (PET)-covered, (McMaster Carr, Catalog Number 8567k52) glass plates sealed with a silicone rubber spacer (≈ 0.1 cm thick). For RAFT and ATRP polymerizations, instead, the mixtures consisted of monomer EA, initiator HMP (0.02 mol %), CTA agent (0.1 mol %), and toluene (10% v/v) and, monomer EA, initiator EBiB (0.07 mol %), catalyst CuBr (0.007 mol %) and ligand Me_6TREN (0.028 mol %), and DMSO (10% v/v), respectively. Notably, the RAFT and ATRP polymerizations were conducted at slightly different concentrations of EBiB and CTA to account for differences in initiation efficiency and afford chain growth at similar concentrations of propagating radicals (see a detailed summary of the polymerization conditions in Table S1 and GPC traces in Figures S1−2). Under these conditions, both mechanisms result in linear polymers with similar average and distributions of molecular weights.

The polymerizations were initiated by irradiating the mixtures with UV light (365 nm, 0.30 mW·cm^{-2}), and the monomer conversions were monitored using ^{1}H NMR spectroscopy. Specifically, reaction aliquots (50 μL) were dissolved in $CDCl_3$ (600 μL), and the spectra were collected in a Bruker Avance 500 MHz spectrometer. The linear polymers were terminated by exposing the polymerization mixtures to atmospheric oxygen. Only the polymer synthesized by ATRP was further purified by eluting a 20% w/v polymer solution in THF over a stationary phase of basic aluminum oxide to remove the CuBr. The THF was evaporated in a rotary evaporator, and the polymers were dried overnight in a vacuum oven equilibrated at 30 °C.

https://doi.org/10.1021/acs.macromol.4c00905
Macromolecules 2024, 57, 8698−8711

The polymers (3.0 mg) were dissolved in HPLC-grade chloroform (2.0 mL) to determine their molecular weight. The resulting polymer solutions were filtered through PTFE (0.45 μm pore size) and eluted through Agilent PLgel 10 μm MIXED-B and 5 μm MIXED-C columns (200−10,000,000 g·mol^{-1} relative to polystyrene standards) using an Agilent 1260 Infinity refractive index detector, a flow rate of 0.5 mL·min^{-1}, and a temperature of 30 °C. Finally, the number-average molecular weight, M_n, and dispersity, $Đ$, were estimated using a calibration curve constructed with polystyrene standards.

Polymerization of Ethyl Acrylate (EA): Filler Networks. Polymer networks were synthesized in a N_2-filled glovebox, following a procedure introduced by Ducrot et al.[50−52] Like in the synthesis of linear polymers, the concentration of propagating radicals was fixed at ≈0.1 mol % through the concentration of initiator (free radical and ATRP) or chain transfer agent (RAFT).

For free radical copolymerizations, monomer EA, cross-linker BDA (0.5−2.0 mol %), and initiator HMP (0.1 mol %) were mixed in a 20 mL scintillation vial and transferred to a mold composed of two PET-covered glass plates sealed with a silicone rubber spacer (≈ 0.1 cm thick). For RAFT and ATRP copolymerizations, instead, the mixture consisted of monomer EA, cross-linker BDA (0.7−2.0 mol %), initiator HMP (0.02 mol %), CTA agent (0.1 mol %), and toluene (10% v/v); and monomer EA, cross-linker BDA (0.7−2.0 mol %), initiator EBiB (0.07 mol %), catalyst CuBr (0.007 mol %), ligand Me_6TREN (0.028 mol %), and DMSO (10% v/v), respectively. Importantly, ATRP copolymerizations were conducted directly on glass, as their kinetics were too slow to prevent diffusion of the EA monomer within the PET sheets and excessive adhesion of the networks (see a detailed summary of the polymerization conditions in Table S2).

The copolymerizations were initiated by irradiating with UV light (365 nm, 0.30 mW·cm^{-2}) and conducted up to ≈100% conversion. That is, 2 h for networks synthesized by free radical polymerization, 24 h for networks synthesized by RAFT, and 48 h for networks synthesized by ATRP, as determined from the kinetics of chain-growth polymerization of EA monomer. The resulting polymer networks were transferred outside the glovebox and dried overnight in a vacuum oven at 30 °C. These networks typically had 8 × 4 × 0.1 cm^3 dimensions and gel fractions above 99%.

Determination of Percolation Thresholds. Percolation thresholds were determined by ^{1}H NMR, taking an aliquot of the viscous copolymerization mixture at the early stages of conversion (i.e., before the gel point), and calculating the monomer conversion from the integrals of the vinyl and backbone peaks. The percolation threshold was defined as the conversion at which the viscous copolymerization mixture turns insoluble in $CDCl_3$, the ^{1}H NMR solvent. More details about the calculations are provided in the SI.

Thermolysis of the Filler Networks. In one of the networks synthesized by RAFT, the trithiocarbonyl groups were removed following a procedure reported Bekanova et al.[53] Briefly, the polymer network was heated to 150 °C under vacuum for 24 h.

Aminolysis of the Filler Networks. In a subset of networks synthesized by RAFT and ATRP, the trithiocarbonyl and bromoisobutyrate groups were removed following procedures reported by Li et al. and Coessens et al.[54,55] Briefly, the polymer networks were swollen in a triethylamine solution (0.02 M in anisole) for 24 h and dried overnight under vacuum at 30 °C.

Polymerization of Ethyl Acrylate (EA): Multiple Networks. Multiple-networks were synthesized in a N_2-filled glovebox following a procedure introduced by Ducrot et al.[50−52] Briefly, polymer networks synthesized by free radical, RAFT, or ATRP were swollen to equilibrium with a solution (40 mL) of monomer EA (99.98 mol %), cross-linker BDA (0.01 mol %), and initiator HMP (0.01 mol %) and transferred to a mold composed of two PET−covered glass plates. The swollen networks were irradiated with UV light (365 nm, 0.30 mW·cm^{-2}) for 2 h until the copolymerization reached ≈100% conversion. The resulting multiple-networks were transferred outside the glovebox and dried overnight in a vacuum oven at 30 °C. Their dimensions were dictated by the swelling ratio, Q, or prestretch, λ_0, of the initial networks and, as demonstrated by Millereau et al., could be finely controlled by incorporating ethyl acetate in the solution used for swelling.[56] Importantly, the gel fractions of the multiple-networks were above 99%.

Visualization of Phase Separation in Filler Networks. Cylindrical specimens of 8 mm diameter were cleaned with ethanol and optical paper and placed on a glass slide. Bright field images were acquired on a Zeiss Axio Scope A1 with a 20X LD Plan − Neofluar objective.

Rheology. Polymer networks were punch-cut into cylindrical specimens of 8 mm diameter, and their rheological properties were evaluated in a Discovery HR-2 rheometer equipped with stainless steel flat plates of 8 mm diameter. Frequency sweeps from 0.1 rad·s^{-1} to 100 rad·s^{-1} at temperatures from 30 to 75 °C were performed within the linear viscoelastic regime at a strain of 0.10%. Master curves for the storage, G', and loss, G'', moduli were constructed by Time−Temperature Superposition, using a reference temperature of 30 °C and horizontal, a_T, and vertical, b_T, shift factors.

Uniaxial Tension. Polymer networks were punch-cut into dog-bone-shaped specimens of 20 mm gauge length and 4 mm width. These specimens were marked with two dots of white paint and deformed with an Instron 34TM5 equipped with a 100 N load cell and a video extensometer at an initial stretch rate of 3×10^{-3} s^{-1} and a temperature of 23 °C. The resulting force−displacement curves were used to compute the engineering stress, $\sigma = F/A$, and stretch, $\lambda = L/L_0$, with F being the measured force, A the specimen cross-sectional area in the undeformed state, and L and L_0 the specimen lengths in the deformed and undeformed configurations, respectively.

The stress−stretch curves were used to estimate the Young's modulus, E, according to

$$E = \left.\frac{d\sigma}{d\lambda}\right|_{\lambda=1.05} \tag{1}$$

The stress−stretch curves of the multiple-networks were fitted to Gent's hyperelastic model to estimate the strain stiffening, λ_m, according to

$$\sigma = \frac{E\left(\lambda - \frac{1}{\lambda^2}\right)}{3\left(1 - \frac{J_1}{J_m}\right)} \tag{2}$$

In this model, $J_1 = \lambda^2 + \frac{2}{\lambda} - 3$ is the first invariant, and $J_m = {\lambda_m}^2 + \frac{2}{\lambda_m} - 3$ is the maximum of the first invariant at the limiting extensibility, λ_m.

Reactive Monte Carlo Simulations. The distribution of elastically active chains, loops, and dangling chains was examined with reactive Monte Carlo simulations using a three-dimensional bond fluctuation model (3DBFM),[57,58] which is detailed in the SI. These simulations were implemented by considering the key elementary steps of free radical copolymerizations and RDRPs. Specifically, for free radical copolymerizations, the simulations accounted for initiation, propagation, and termination, with rate constants k_i, k_p, and k_t related by $k_t > k_p \gg k_i$.[59] For ATRP copolymerizations, the simulations only accounted for propagation, with $k_i = k_t = 0$ due to the negligible concentration of propagating radicals resulting from reversible termination (i.e., the simulation did not consider initiation and termination).[60] Finally, for RAFT copolymerizations, the simulations accounted for propagation and termination, with $k_p \gg k_t$. After all, in these copolymerizations, reversible deactivation occurs by chain transfer to a trithiocarbonate chain transfer agent, and the concentration of propagating radicals is not negligible.

Two critical assumptions were made in the simulations. First, the activation and deactivation reactions were treated implicitly because the equilibrium state of such reversible exchange reactions is readily established at the beginning of the copolymerizations (i.e., at low conversions), and the exchange between the dormant and active species is fast throughout the entire range of conversions.[61,62] Second, the difunctional cross-linker was assumed to propagate in two steps,

https://doi.org/10.1021/acs.macromol.4c00905
Macromolecules 2024, 57, 8698−8711

with propagation rate constants, $k_{p,1} = 2k_{p2}$, that are in agreement with Gao et al.[63]

The architecture of the simulated networks was used to estimate the distribution of elastically active chains and topological defects such as loops and dangling chains. The elastically active chains, loops, and dangling chains were defined as unique paths between two cross-linkers, a chain end and a cross-linker, and a cross-linker onto itself, respectively. Notably, the units along the elastically active chains, loops, and dangling chains had a functionality, $f = 2$, in agreement with the one-dimensional character of linear polymers.

The architecture of the simulated networks was also used to estimate the percolation threshold from the reduced degree of polymerization (i.e., the degree of polymerization without accounting for the largest macromolecule in the ensemble). Details of this estimation are provided in the SI; briefly, the percolation threshold was defined as the double bond conversion at which the weight-average degree of polymerization, DP_w, was maximized upon exclusion of the longest chain. This definition is similar to that used by Gao et al. in a seminal contribution on the role of living copolymerizations on gelation.[63]

RESULTS AND DISCUSSION

RDRPs Offer Control over the Kinetics of Chain Growth Polymerization and the Molecular Weight Distribution of Linear Polymers. Both conventional free radical polymerization and RDRPs proceed through initiation, propagation, and termination of chain ends. However, the mechanisms drastically differ in the presence of reversible deactivation steps. In RDRPs, active radicals can reversibly terminate or chain transfer and are less likely to combine or disproportionate into "dead" chains, leading to linear polymers of narrow dispersity and well-defined molecular weight (see Scheme 1).

Scheme 1. The main difference between Free Radical Polymerizations and RDRPs is the presence of elementary steps that reversibly deactivate the propagating radicals. These steps slow down the polymerization and allow for the synthesis of linear polymers with narrow dispersity and well-defined molecular weight. The two RDRPs, RAFT and ATRP, differ in their reversible deactivation step, which involves fragmentation of a chain transfer agent in RAFT and electron transfer to a copper-ligand catalyst in ATRP

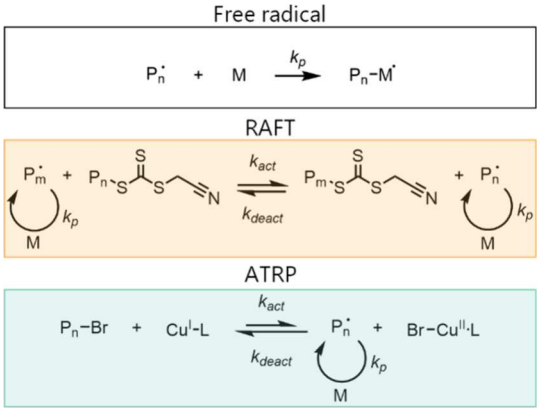

Among RDRP techniques, RAFT and ATRP are the two most common. Both polymerizations involve a reversible deactivation step but are inherently different. RAFT polymerizations rely on reversible chain transfer through the reaction of an active radical with a chain transfer agent.[64] In contrast, ATRPs depend on reversible termination of an active radical with a copper-ligand catalyst.[65] Reversible chain transfer does not affect the active radical concentration such that RAFT polymerizations typically proceed at faster rates than ATRPs and have a higher probability of termination. However, RAFT polymerizations are still slower than conventional free radical polymerizations due to "retardation" effects that remain to be understood.[64,66−71]

To highlight the role of the polymerization mechanism on the kinetics of chain growth, we synthesized three linear polymers by free radical, RAFT, and ATRP polymerization of ethyl acrylate monomer. The polymerizations were conducted in bulk or concentrated solution (90 vol %) and initiated by UV, maintaining the concentration of growing chain ends constant at 0.1 mol % or, in other words, the target molecular weight at $M_n \approx 100$ kDa. The concentration of growing chain ends was controlled through the chain transfer agent and organic halide initiator in RAFT and ATRP polymerizations, as well as the radical photoinitiator in the free radical. However, the control over this concentration was poor in the free radical polymerization due to the excessive number of chain termination events that occur throughout the polymerization (see detailed synthetic conditions in the Materials and Methods section).

Consistent with the outlined differences in polymerization mechanisms, the rate of polymerization was comparable in free radical and RAFT polymerizations and considerably slower in ATRP (see monomer consumption over time in Figure 1A and apparent rate constants in Table 1). The RAFT and ATRP

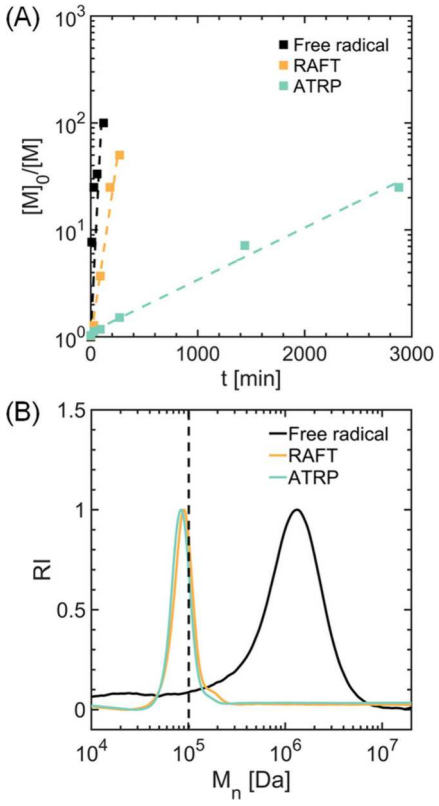

Figure 1. Chain growth polymerization of linear poly(ethyl acrylate) chains. (**A**) The rate of polymerization is comparable in free radical and RAFT polymerizations but significantly slower in ATRP. (**B**) A reversible deactivation step in RAFT and ATRP polymerizations results in linear polymers of narrow dispersity and (dashed line) target molecular weight.

https://doi.org/10.1021/acs.macromol.4c00905
Macromolecules 2024, 57, 8698−8711

Table 1. Apparent rate constant, k_{app}, for Free Radical, RAFT, and ATRP polymerizations, and molecular weight, M_n, and dispersity, $Đ$, of the resulting linear polymer chains

Mechanism	k_{app} [min^{-1}]	M_n [kDa]	$Đ$
Free radical	0.05	1100	1.9
RAFT	0.02	96	1.1
ATRP	0.001	90	1.1

polymerizations resulted in linear polymers with narrow dispersity, $Đ \approx 1.1$, and target molecular weight, $M_n \approx 100$ kDa. In contrast, the free radical polymerization resulted in polymers of broader $Đ \approx 1.9$ and higher $M_n \approx 1100$ kDa (see GPC traces in Figure 1B).

RDRPs Result in Higher Percolation Thresholds, Phase Separation, and Softer Polymer Networks. We synthesized three polymer networks by free radical, RAFT, and ATRP copolymerizations of ethyl acrylate monomer and 1,4-butanediol diacrylate cross-linker. Similar to the synthesis of the linear polymers, the copolymerizations were conducted in bulk or concentrated solution (90 vol%) and initiated by UV, keeping the radical and cross-linker concentration at 0.1 and 1.0 mol %, respectively (see detailed synthetic conditions in the Materials and Methods section). The free radical, RAFT, and ATRP copolymerizations were conducted for 2, 24, and 48 h to attain complete conversion and resulted in polymer networks with gel fractions of more than 99 wt %.

The first interesting observation relates to the vinyl group conversion at which the monomer-cross-linker mixtures underwent gelation. This conversion was considered as the percolation threshold and was 5, 20, and 40% for the free radical, RAFT, and ATRP copolymerizations, respectively (see Figure 2B). Second, upon complete conversion (gel fraction of 99 wt %), the optical appearance of the networks was remarkably different. Networks synthesized by RAFT and ATRP were (i) bright yellow or pale green due to the presence of chain transfer agent or copper-ligand catalyst and (ii) opaque (see pictures in Figure 2A and transmittance spectra of specimens with a thickness of ≈1 mm in Figure 2C). Third, the networks synthesized by RAFT and ATRP were softer than the analogue synthesized by free radical copolymerization, with a lower tensile modulus, $E_{RDRPs} \approx 0.8$ MPa vs $E_{FRP} \approx 1.2$ MPa (see stress−stretch curve in Figure 2D, and storage and loss moduli in Figure S10B). Finally, the network synthesized by free radical copolymerization had similar percolation threshold and mechanical properties to a control network synthesized in the presence of an irreversible chain transfer agent, 1-octanethiol, at 0.1 mol %; conditions that lead to linear polymers with molecular weights similar to those obtained by RAFT and ATRP, $M_n \approx 130$ kDa (see GPC trace, percolation threshold, and stress−stretch curve in Figure S3). Overall, these observations indicate that RDRP copolymerizations result in higher percolation thresholds, phase separation, and softer polymer networks.

RDRPs Lower the Rate of Cluster Growth and Lead to Higher Percolation Thresholds. To better understand the effect of RDRPs on gelation, we varied the nominal concentration of 1,4-butanediol diacrylate cross-linker from 0.7 to 2.0 mol % in the free radical, RAFT, and ATRP copolymerizations, maintaining the concentration of radicals at 0.1 mol % (see detailed synthetic conditions in the Materials and Methods section). In free radical copolymerizations, the

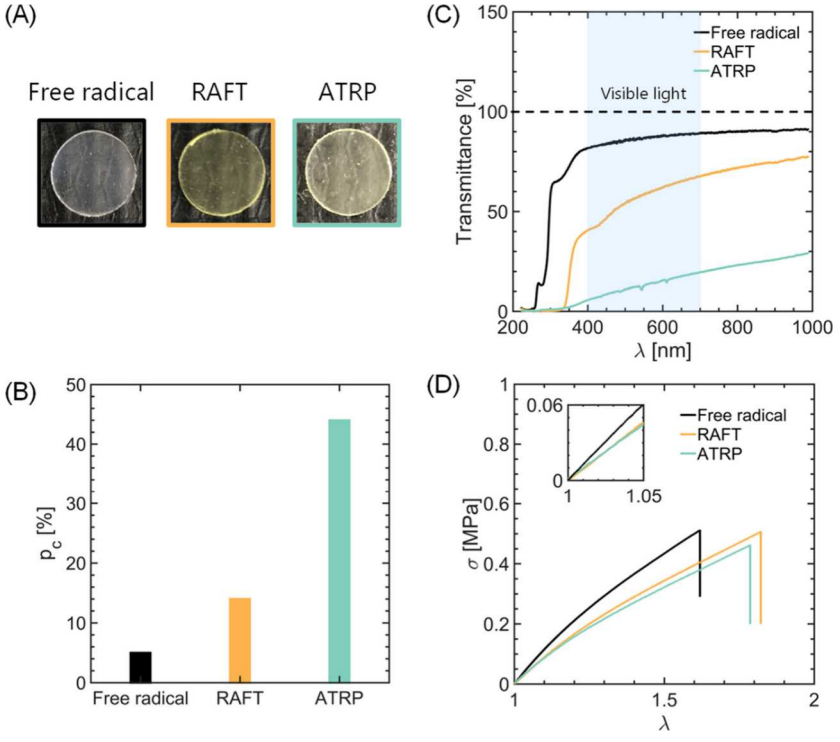

Figure 2. Critical features of polymer networks synthesized by free radical and RDRP copolymerizations. (**A**) Polymer networks synthesized by free radical copolymerizations are transparent. In contrast, analogues synthesized by RAFT and ATRP are bright yellow and pale green due to the presence of a chain transfer agent and copper-ligand catalyst. RDRPs lead to higher percolation thresholds, phase separation, and softer and more extensible networks. These features are illustrated by the (**B**) vinyl group conversion at which the monomer-cross-linker mixtures percolate into networks, the (**C**) transmittance spectra of specimens with ≈1 mm thickness, and the (**D**) stress−strain curves in uniaxial tension.

https://doi.org/10.1021/acs.macromol.4c00905
Macromolecules 2024, 57, 8698−8711

percolation thresholds were insensitive to the cross-linker concentration, $p_c \approx 5\%$. In contrast, in RAFT and ATRP copolymerizations, the percolation thresholds decreased from 30 to 15% and 45 to 10%, respectively (see Figure 3),

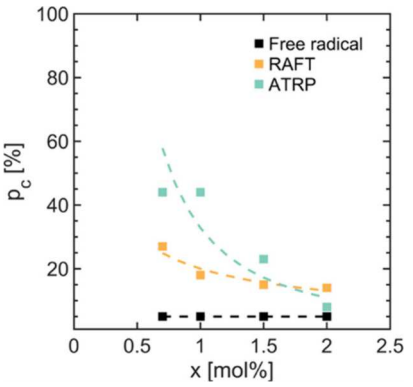

Figure 3. Percolation thresholds in bulk copolymerizations. Free radical copolymerizations percolate at lower conversions than RDRPs due to the lack of a chain transfer agent or copper-ligand catalyst to reversibly deactivate the propagating radicals.

indicating that free radical copolymerizations have lower percolation thresholds than RAFT and ATRP copolymerizations irrespective of the cross-linker concentrations. These observations are in agreement with previous work from Fukuda, Zhu, Bannister and Armes, Cochran, Matyjaszewski, and others,[41,42,72−75] and also highlight that ATRP copolymerizations have percolation thresholds that depend more notably on the cross-linker concentration than RAFT copolymerizations.

We gained mechanistic insights into these observations by conducting reactive Monte Carlo (MC) simulations based on a three-dimensional bond fluctuation model (3DBFM),[57,58] briefly described in the Materials and Methods section and detailed in the SI. In this model, monomers and cross-linkers react to form clusters at low conversions, and these clusters interconnect into a network at the percolation threshold. A key parameter governing the percolation threshold is the rate of cluster growth, which depends on the probability of forming a covalent bond via radical propagation or combination. Hence, this rate was evaluated in free radical copolymerizations and RDRPs by conducting MC simulations at various cross-linker concentrations. Notably, free radical copolymerizations featured higher cluster growth rates than RDRPs at the same vinyl group conversion, in agreement with their mechanisms of copolymerization (see cluster size distributions in Figure 4A−C, noting the scale differences in the *x*- and *y*-axes, and Figures S26−28). Specifically, in the absence of chain transfer agents or copper-ligand catalysts, radicals initiate slowly and propagate rapidly to form a few clusters that grow quickly until the gel point. In contrast, in the presence of chain transfer agents or copper-ligand catalysts, radicals initiate rapidly and propagate slowly to form clusters that grow steadily until percolation. As a result, free radical copolymerizations exhibit lower percolation thresholds than RDRPs over the entire range of cross-linker concentrations (see estimates of the percolation

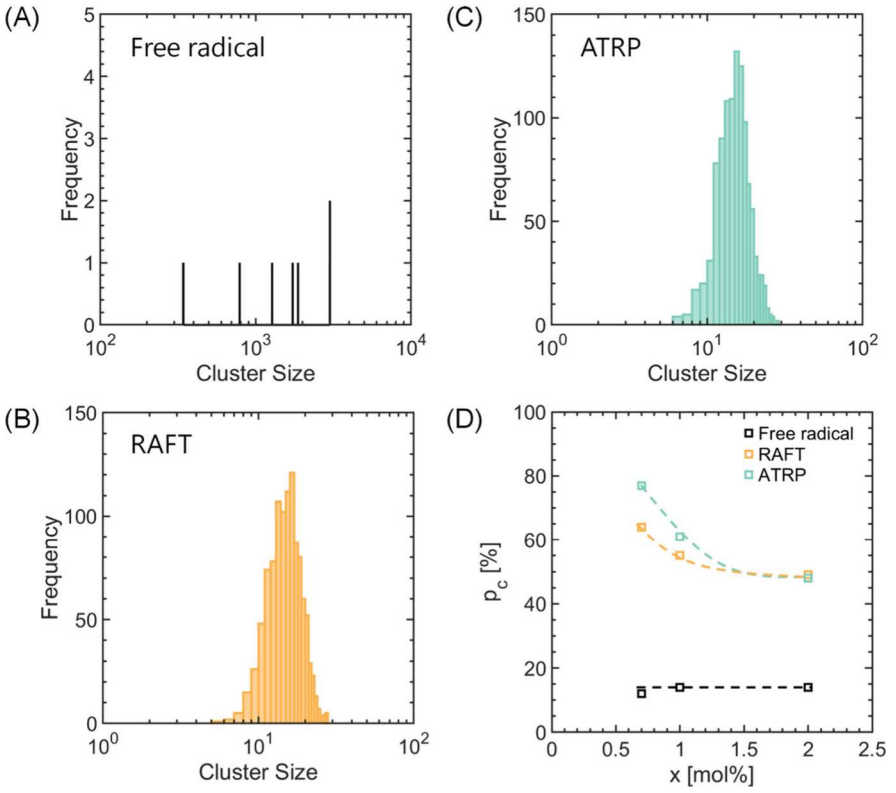

Figure 4. Reactive Monte Carlo simulations of free radical and RDRP copolymerizations. (**A−C**) At low vinyl group conversions, 3%, and similar cross-linker concentrations, 1.0 mol %, free radical copolymerizations feature fewer and more rapidly growing clusters than RDRP copolymerizations because of their lower rates of radical initiation and higher rates of radical propagation and termination. This difference in copolymerization mechanism leads to lower (**D**) percolation thresholds in free radical copolymerizations.

https://doi.org/10.1021/acs.macromol.4c00905
Macromolecules 2024, 57, 8698−8711

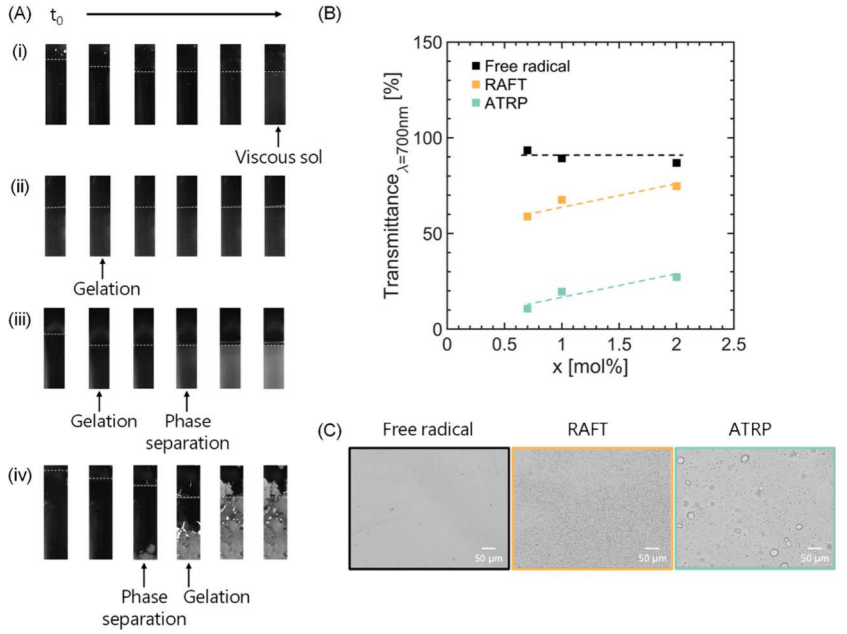

Figure 5. Monomer-cross-linker copolymerizations unveil an interplay between gelation and phase separation. (**A**) We observe four different behaviors: (i) cross-linking without gelation, (ii) instantaneous gelation, (iii) gelation before phase separation, and (iv) phase separation before gelation. Phase separation results in more opaque networks, as measured by the (**B**) transmittance to 700 nm light and imaged under (**C**) brightfield optical microscope.

Scheme 2. RDRP copolymerizations lead to phase separation after gelation, crosslink Localization, and softer and more swellable polymer networks

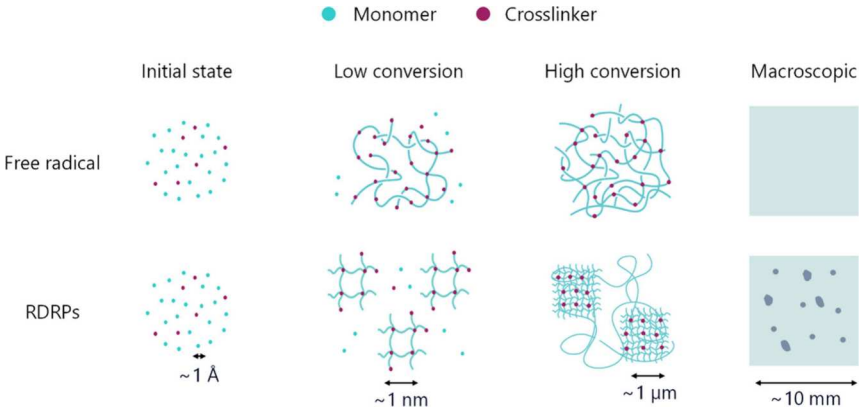

threshold from reactive Monte Carlo simulations in Figure 4D).

RAFT and ATRP copolymerizations are seen to lead to different percolation thresholds, especially at low cross-linker concentrations. Both reactions feature reversible deactivation, fast initiation, and slow propagation, but RAFT copolymerizations have higher probabilities of chain termination. Thus, at the same vinyl group conversion, RAFT copolymerizations have higher cluster growth rates and lower percolation thresholds than analogues conducted by ATRP (see slight differences in the cluster size distributions in Figure 4B−C and Figures S26−28 and estimates of the percolation threshold from reactive Monte Carlo simulations in Figure 4D and Figure S25).

Notably, while reactive Monte Carlo simulations qualitatively describe gelation in free radical, RAFT, and ATRP copolymerizations, the percolation thresholds differ from those measured experimentally. This quantitative discrepancy is attributed to the implicit account of reversible deactivation in the simulations, which hinders the ability to capture fluctuations in the radical concentration and their impact on the percolation threshold. Moreover, the rate constants in the reactive Monte Carlo simulations were not optimized to exactly mimic the specific copolymerizations under consideration.

RDRPs Lower the Rate of Cluster Growth and Lead to Phase Separation during Gelation. To gain insights into the opaqueness of the polymer networks, we monitored the optical appearance of the monomer-cross-linker mixtures throughout the copolymerizations and, remarkably, observed four different behaviors. The first was cross-linking without gelation, observed in RDRP copolymerizations conducted at cross-linker concentrations lower than 0.7 mol %. The second was instantaneous gelation, observed in free radical copolymerizations at every cross-linker concentration. The third was gelation before phase separation, observed in RDRP

https://doi.org/10.1021/acs.macromol.4c00905
Macromolecules 2024, 57, 8698−8711

copolymerizations conducted at cross-linker concentrations from 0.7 to 2.0 mol %. And the fourth was phase separation before gelation, observed in ATRP copolymerizations conducted above a cross-linker concentration of 5 mol % (see representative images of the four behaviors in Figure 5A).

The emergence of phase separation during gelation has significant consequences for the optical properties of the networks. Specifically, polymer networks formed by instantaneous gelation (i.e., synthesized by free radical copolymerization) were translucent and had a transmittance to 700 nm light insensitive to the cross-linker concentration, $T\% \approx 90\%$. Instead, polymer networks that underwent phase separation after gelation (i.e., synthesized by RDRP copolymerizations) were opaque and had a transmittance to 700 nm light that increased from 60 to 75% and from 10 to 30% with the cross-linker concentration of RAFT and ATRP copolymerizations, respectively (see transmittance at 700 nm in Figure 5B, and transmittance spectra in Figure S5). The structure of these networks consisted of μm-size clusters embedded within a polymer matrix, as imaged by brightfield optical microscopy (see images in Figure 5C and Figures S6−7, and Scheme 2).

Together, our observations highlight an important point. RDRP copolymerizations offer more mesoscopically heterogeneous polymer networks than free radical copolymerizations when conducted in bulk. The formation of covalent bonds by radical propagation or combination gives rise to excluded volume interactions that can drive phase separation before or after gelation, even in an athermal copolymerization like that of ethyl acrylate monomer and 1,4-butanediol diacrylate cross-linker.[10,11,29,38] In the presence of chain transfer agents or copper-ligand catalysts, the probability of forming covalent bonds decreases, the percolation threshold shifts to higher vinyl group conversions, and the excluded volume interactions can be sufficiently strong to drive phase separation. As described by Dušek,[29,30] the network might experience microsyneresis around the percolation threshold, with regions enriched in cross-linked polymer locally expelling unreacted monomer and cross-linker and forming mesophases of cross-linker-rich and cross-linker-poor domains. In principle, the interplay between the probability of forming a covalent bond, the percolation threshold, and phase separation could be controlled through the concentration of chain transfer agent or copper-ligand catalyst. However,the details of such control are beyond the scope of this work. We believe they are essential to understand given the recent body of work on how RDRPs offer more homogeneous networks than free radical copolymerizations, i.e., a more homogeneous distribution of chain lengths.[41,47,48,73,76]

Two control experiments further support this point. The first relates to a network synthesized by free radical copolymerization at the same toluene and DMSO concentrations (10% v/v) used in RDRPs. This network was transparent to visible light due to the high probability of forming covalent bonds upon radical propagation (see Figure S7). The second involves a network synthesized by free radical copolymerization at very low initiator concentrations, 0.0004 mol %. This network was opaque and had $T\% \approx 59\%$ due to the low probability of forming covalent bonds at such low radical concentrations (see Figure S8).

RDRPs Lead to Softer and More Swellable Polymer Networks. Having discussed the effect of RDRPs on the mesoscopic structure of polymer networks, we now focus on the bulk physical properties, noting that both free radical and RDRP copolymerizations were conducted to complete conversion in bulk or concentrated solution and resulted in networks with ≈99% gel fractions and glass transition temperatures, $T_g \approx -18$ °C (see thermograms in Figure S4). We first considered the tensile modulus, which was ≈30% lower in networks synthesized by RDRP at nominal cross-linker concentrations from 0.7 to 2.0 mol % (see Figure 6A),

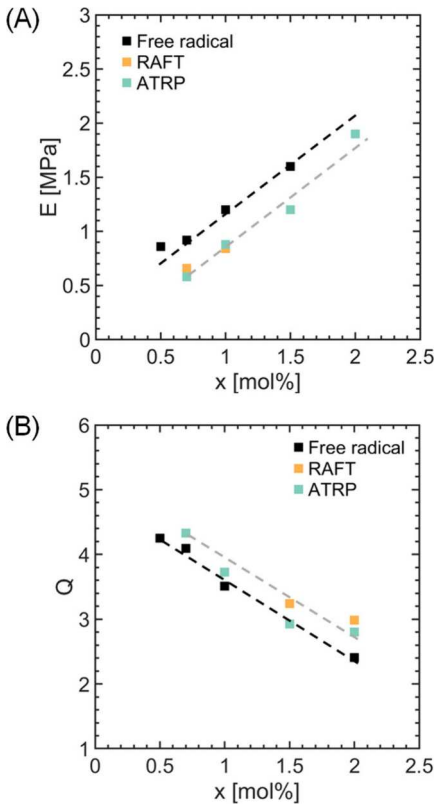

Figure 6. Physical properties of polymer networks synthesized by RDRP and free radical copolymerizations. (**A**) Young's modulus in uniaxial tension. (**B**) Equilibrium swelling ratio in an athermal solvent like ethyl acrylate.

and approximately equal to three times the storage modulus, $E = 3G'$ (see storage and loss moduli in Figure S10 and stress−stretch curves in Figure S11). Then, we examined the equilibrium swelling ratio, Q, which, in an athermal solvent like ethyl acrylate monomer, was ≈10% higher in networks synthesized by RDRPs over the entire range of cross-linker concentrations (see Figure 6B). Together, these observations indicate that RDRPs lead to softer and more swellable polymer networks than free radical copolymerizations.

Two effects could contribute to this behavior. The first is molecular and relates to the impact of RDRP copolymerizations on the density of elastically active chains. To examine this impact, we estimated the density of elastically active chains using reactive Monte Carlo simulations and unveiled that, at 98% vinyl group conversion, this density was lower in networks synthesized by RDRPs than by free radical copolymerization at every cross-linker concentration (see estimates of the cross-link density in Figure 7 and the corresponding Young's modulus in Figure S31). Moreover, we examined the mechanical properties of two control polymer networks synthesized by free radical and RAFT copolymerizations at a cross-linker concentration of 20 mol %. These networks were homoge-

https://doi.org/10.1021/acs.macromol.4c00905
Macromolecules 2024, 57, 8698−8711

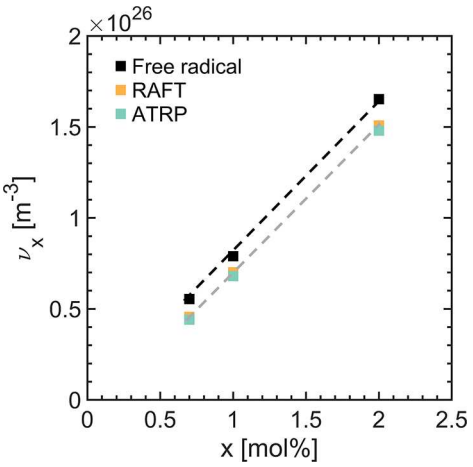

Figure 7. Density of elastically active chains in polymer networks synthesized by RDRP and free radical copolymerizations, as estimated from reactive Monte Carlo simulations.

neous (i.e., optically translucent with a transmittance of $T\% \approx 90\%$) but still had different mechanical properties. Specifically, the network synthesized by RAFT copolymerization was still softer than that synthesized by free radical copolymerization, indicating that, beyond shifting the percolation threshold to higher vinyl group conversions, RDRP copolymerizations do affect the connectivity of the polymer chains at the molecular scale (see rubbery plateau in storage modulus, E', in Figure S9).

The second effect is mesoscopic and pertains to the role of phase separation on the spatial distribution of chains within the networks. To examine this effect, we evaluated the mechanical properties of two control polymer networks synthesized by free radical copolymerization, controlling the rate of gelation by decreasing the initiator concentration from 0.1 to 0.0004 mol %. These networks were homogeneous (i.e., optically translucent) and heterogeneous (i.e., opaque with a transmittance of $T\% \approx 59\%$), respectively, but, remarkably, had the same tensile modulus, E, and mechanical properties (see stress−stretch curve in Figure S8).

Collectively, these observations led us to conclude that the differences in mechanical properties between networks synthesized by free radical and RDRP copolymerizations primarily stem from the molecular connectivity of the polymer chains rather than from the emergence of mesophases during gelation.

RDRPs Lead to a Different Interplay between Small- and Large-Strain Mechanical Properties. To examine the impact of RDRPs on the large-strain mechanical properties, we swelled the polymer networks in a solution of ethyl acrylate monomer, 1,4-butanediol diacrylate cross-linker (0.01 mol %), and 2-hydroxy-2-methylpropiophenone initiator (0.01 mol %), and then initiated polymerization with UV light (see Scheme 3). Details of this procedure are provided in the Materials and Methods sections, but, in essence, we embedded the polymer networks synthesized by free radical, RAFT, and ATRP copolymerizations within a multiple-network architecture like that introduced by Gong and Creton in hydrogels and elastomers, respectively.[50,77] Three features of these multiple-networks are worth noting. First, their architecture, which consists of a filler network chemically interconnected to a matrix network due to transfer or reinitation reactions between propagating radicals and trithiocarbonyl, bromoisobutyrate, or

Scheme 3. Synthesis of multiple-networks by swelling and copolymerization. Swelling polymer networks with an athermal solvent like ethyl acrylate pre-stretches their chains closer to their contour length

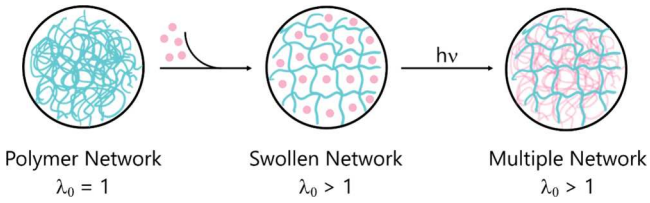

other reactive groups (e.g., C−H bonds). Second, their toughness due to filler network scission.[50,78] And third, their strain-stiffening at moderate-to-large deformations due to filler network chains elongating near their limiting extensibility or contour length. This third feature results in stress−stretch curves that collapse onto a master curve when renormalized by the swelling ratio, Q, or filler network prestretch, $\lambda_0 = Q^{1/3}$, according to $\sigma \rightarrow \sigma\lambda_0^2$ and $\lambda \rightarrow \lambda\lambda_0$.[56,79] Thus, we used these multiple-networks to probe the large-strain mechanical properties of polymer networks that were too brittle in their solvent-free or swollen states to sustain large deformations.

We examined the limiting extensibility of two families of polymer networks. The first was based on polymer networks synthesized by free radical, RAFT, and ATRP copolymerizations at the same nominal cross-linker concentration, 1.0 mol %. This family of polymer networks had the stress−stretch curves, mesoscopic structure, and storage and loss moduli depicted in Figure 2D, Figure 5C, and Figure S10B, and led to multiple-networks with a strain stiffening governed by the prestretch of the filler network chains, λ_0 (see individual stress−stretch curves in Figure S17 and master curve in Figure S15B). We estimated the limiting extensibility of the filler network chains, $\lambda_h = \lambda_m\lambda_0$, by considering the stress−stretch curves of the multiple-networks within a Gent hyperelastic model to obtain the maximum of the first invariant, $J_m = \lambda_m^2 + 2/\lambda_m - 3$, and limiting extensibility of the multiple-network chains, λ_m (see details of these estimates in the Materials and Methods section and fits of the stress−stretch curves in Figure S17). Interestingly, the polymer network synthesized by free radical copolymerization was slightly less extensible than the analogues synthesized by RDRPs, with limiting extensibilities $\lambda_{h,FR} = 3.5 \pm 0.2$ vs $\lambda_{h,RDRP} \approx 3.8 \pm 0.2$. This observation was in line with molecular elasticity and swelling theories, which predict a trade-off between elasticity, E, and limiting extensibility of the polymer chains, λ_h (typically represented as the molecular weight between cross-links, M_x).[80] In addition, it was consistent with our reactive Monte Carlo simulations, which yielded a higher density of short elastic chains (i.e., shorter than the average) in the network synthesized by free radical copolymerization than in the ones synthesized by RDRPs (see distribution of elastically active chains in Figure S29B). And finally, it was insensitive to the presence of trithiocarbonyl or bromoisobutyrate groups in the filler network, as networks synthesized by RAFT and ATRP had a limiting extensibility of $\lambda_{h,RDRP} = 3.8$ even after these groups were removed by thermolysis or aminolysis (see stress-strech curves Figure S20 and summary of the mechanical properties in Table S4).

A more interesting observation relates to the second family of polymer networks, which was based on networks

https://doi.org/10.1021/acs.macromol.4c00905
Macromolecules 2024, 57, 8698−8711

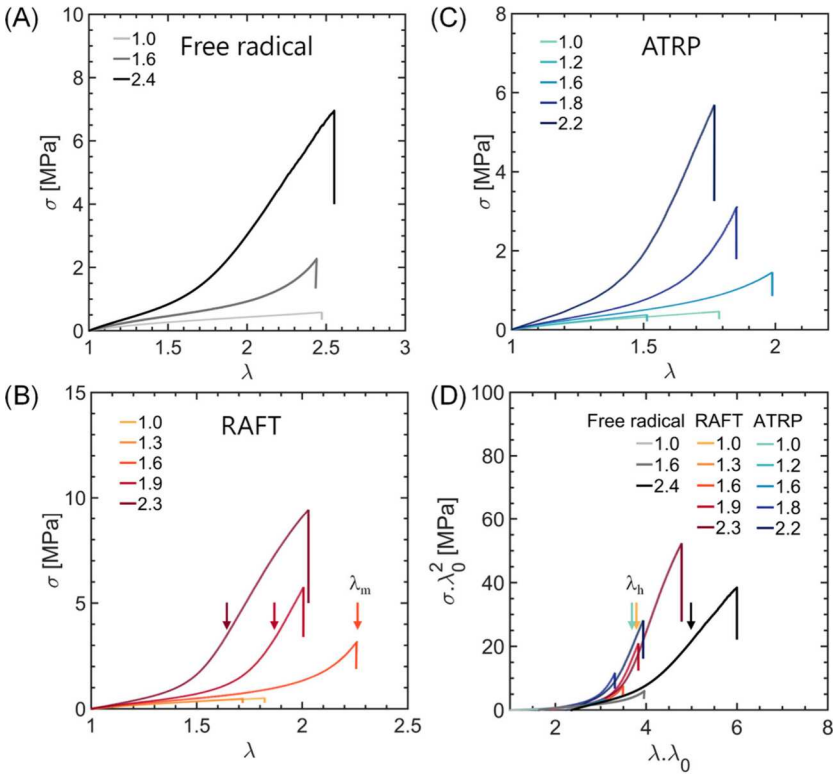

Figure 8. Mechanical properties of multiple networks composed of filler networks synthesized by (**A**) free radical, (**B**) RAFT, and (**C**) ATRP copolymerizations. These filler networks have the same Young's modulus, $E \approx 0.86$ MPa, as depicted in Figure S19. The arrows indicate the position of the strain hardening, λ_m. (**D**) Renormalizing the stress−stretch curves by the filler network prestretch, λ_0, unveils drastic differences in the large-strain mechanical properties. Specifically, the polymer networks synthesized by RDRPs strain stiffen at a lower stretch because their chains are, on average, less extensible. The arrows indicate position of the limiting extensibility of the filler network chains, λ_h.

synthesized by free radical, RAFT, and ATRP copolymerization at different cross-linker concentrations (0.5 mol % for the free radical polymerization and 1.0 mol % for the RDRPs). These networks had the same modulus, E, swelling ratio, Q, and prestretch of the filler network chains, λ_0, and were indistinguishable from one another within molecular elasticity and swelling theories. Namely, they theoretically had the same density of elastically active chains. However, when incorporated within multiple-networks, the stress−stretch curves revealed that such networks were drastically different at large strains. The network synthesized by free radical copolymerization was more extensible than the analogues synthesized by RDRPs, with limiting extensibilities $\lambda_{h,FR} = 5.0 \pm 0.1$ vs $\lambda_{h,RDRP} = 3.8 \pm 0.2$ (see stress−stretch curves in Figure 8A−C and master curve in Figure 8D). This observation was also consistent with our reactive Monte Carlo simulations, which revealed that the network synthesized by free radical copolymerization had a lower fraction of short elastic chains (see distribution of elastically active chains in Figure 9).

Our observations highlight an important point. Polymer networks synthesized by free radical, RAFT, and ATRP copolymerizations can have the same density of elastically active chains but different distributions of chain lengths at the molecular scale. This difference in molecular architecture means that the networks exhibit a different trade-off between their elasticity and strain stiffening or, namely, between their small- and large-strain mechanical properties. Specifically, networks synthesized by free radical copolymerization obey $\lambda_h \sim E^{-0.7}$ whereas networks synthesized by RDRP, instead, obey $\lambda_h \sim E^{-0.4}$ (see Figure 10).

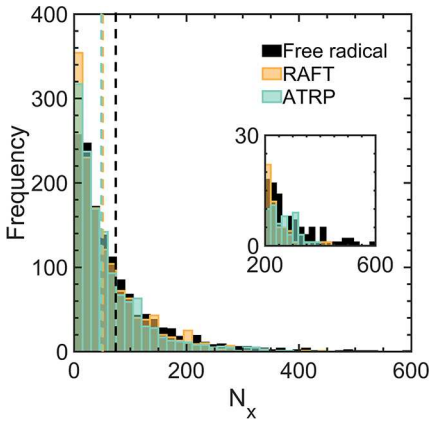

Figure 9. Distributions of elastically active chains in networks synthesized by free radical and RDRP copolymerizations. At similar densities of elastically active chains, $\nu_{x,FRP} = 7.1 \times 10^{25}$ chains·m^{-3} and $\nu_{x,RDRP} = 7.0 \times 10^{25}$, the distributions of the RDRPs and free radical copolymerizations exhibit different mean (dashed) and standard deviations of chain lengths.

CONCLUSIONS

We have investigated the effect of RDRPs on the gelation, phase separation, and mechanical properties of polymer networks. The reversible deactivation of propagating radicals through reaction with a chain transfer agent or copper ligand catalyst lowers the cluster growth rate and strengthens the excluded volume interactions that drive phase separation during gelation. As a result, under similar reaction conditions,

https://doi.org/10.1021/acs.macromol.4c00905
Macromolecules 2024, 57, 8698−8711

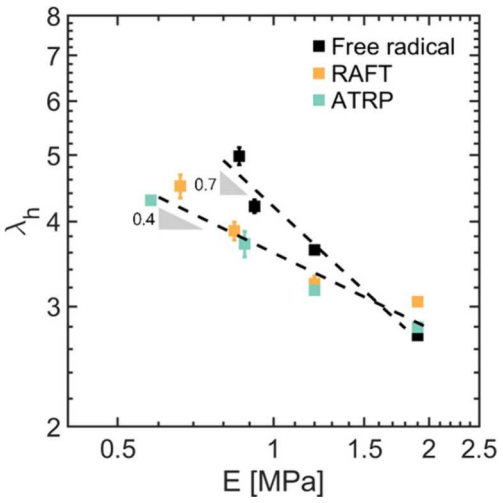

Figure 10. Trade-off between onset of strain stiffening, λ_h, and tensile modulus, E, in networks synthesized by free radical copolymerizations and RDRPs.

RDRPs percolate at higher vinyl group conversions, are more prone to suffer from phase separation, and result in more opaque polymer networks than conventional free radical copolymerizations.

At similar cross-linker concentrations, polymer networks synthesized by RDRPs are softer, more swellable, and more extensible than analogues synthesized by free radical copolymerizations, comprising a lower density of elastically active chains. Instead, at similar densities of elastically active chains, polymer networks synthesized by RDRPs have the same elasticity and swelling ratio as those synthesized by free radical copolymerization but, remarkably, lower extensibilities. Thus, RDRPs offer control over the molecular architecture of polymer networks and, in turn, over their small- and large-strain mechanical properties.

Our results have important implications for polymer science. First, they pave the way for synthesizing model networks for understanding fracture, where the stress states in the bulk and the crack front are governed by the small- and large-strain mechanical properties, respectively. Second, they highlight that, in contrast to the case of linear polymers, RDPRs might offer more heterogeneous polymer networks than free radical copolymerizations due to phase separation during gelation. The materials might have narrower distributions of chain lengths at the molecular scale, but can still develop cross-linker-rich and cross-linker-poor mesophases near the percolation threshold, just like in other networks.[29,81] Finally, they provide a molecular rationale for some of the challenges that emerge when using RDRPs to manufacture three-dimensional objects or parts[82] or structurally tailor and engineer polymer networks[48] These copolymerizations are too slow to prevent phase separation at low cross-linker concentrations and afford networks that are too cross-linked to be elastic and resist fracture at high cross-linker concentrations (i.e., glassy networks). New techniques that afford high rates of copolymerization and controlled molecular architectures are essential for leveraging the interplay between phase separation and gelation and, as such, developing advanced polymer networks.

■ ASSOCIATED CONTENT

Data Availability Statement

All data needed to evaluate the conclusions are present in the paper and/or the Supporting Information, as well as in the Texas Data Repository at 10.18738/T8/SGLQMD

Supporting Information

The Supporting Information is available free of charge at https://pubs.acs.org/doi/10.1021/acs.macromol.4c00905.

> Synthesis of linear polymers, kinetics of RDRPs, synthesis, glass transition, optical properties, phase separation of polymer networks, small- and large-strain mechanical properties of polymer networks synthesized at similar cross-linker concentrations, small- and large-strain mechanical properties of polymer networks composed of similar densities of elastically active chains, summary of mechanical properties, reactive Monte Carlo simulations, and models and calculations (PDF)

■ AUTHOR INFORMATION

Corresponding Author

Gabriel E. Sanoja − *McKetta Department of Chemical Engineering, The University of Texas at Austin, Austin, Texas 78712, United States;* orcid.org/0000-0001-5477-2346; Email: gesanoja@che.utexas.edu

Authors

Aaliyah Z. Dookhith − *McKetta Department of Chemical Engineering, The University of Texas at Austin, Austin, Texas 78712, United States;* orcid.org/0000-0003-4219-5515

Zidan Zhang − *McKetta Department of Chemical Engineering, The University of Texas at Austin, Austin, Texas 78712, United States;* orcid.org/0000-0002-6909-8742

Venkat Ganesan − *McKetta Department of Chemical Engineering, The University of Texas at Austin, Austin, Texas 78712, United States;* orcid.org/0000-0003-3899-5843

Complete contact information is available at: https://pubs.acs.org/10.1021/acs.macromol.4c00905

Author Contributions

Research was designed by A.Z.D., Z.Z., V.G., and G.E.S. Synthesis, mechanical characterization, and optical imaging were conducted by A.Z.D., and data interpreted by A.Z.D. and G.E.S. Reactive Monte Carlo simulations were conducted by Z.Z. and the data interpreted by Z.Z. and V.G. The manuscript was written by A.Z.D., Z.Z., V.G., and G.E.S, and critically revised by all authors. All authors have given final approval to the final version.

Funding

This work was funded by The University of Texas at Austin. V.G. acknowledges partial support from the Welch Foundation (F-1599), the donors of the American Chemical Society Petroleum Research Fund (66812-ND7), and the National Science Foundation (DMR-2225167). The authors acknowledge the Texas Advanced Computing Center (TACC) for the generous allocation of computing resources.

Notes

The authors declare no competing financial interest.

■ ACKNOWLEDGMENTS

We gratefully acknowledge Keldy Mason for support in measuring the light transmittance of the polymer networks. Also, we thank Adrianne Rosales, Ralm Ricarte, Thomas Truskett, and Costantino Creton for their helpful discussions.

■ REFERENCES

(1) Gent, A. N. Engineering with Rubber. In *Engineering with Rubber*; Gent, A. N., Ed.; Carl Hanser Verlag GmbH & Co. KG: München, 2012; pp I−XVIII. .
(2) *Hydrogels in Medicine and Pharmacy*; Peppas, N. A., Ed.; CRC Press, 2019. .
(3) Creton, C. Pressure-Sensitive Adhesives: An Introductory Course. *MRS Bull.* **2003**, *28* (6), 434−439.
(4) Flory, P. J. *Principles of Polymer Chemistry*; Cornell University Press: New York, 1953.
(5) Zhong, M.; Wang, R.; Kawamoto, K.; Olsen, B. D.; Johnson, J. A. Quantifying the Impact of Molecular Defects on Polymer Network Elasticity. *Science (80-.)* **2016**, *353* (6305), 1264−1268.
(6) Wang, R.; Alexander-Katz, A.; Johnson, J. A.; Olsen, B. D. Universal Cyclic Topology in Polymer Networks. *Phys. Rev. Lett.* **2016**, *116* (18), No. 188302.
(7) Rebello, N. J.; Beech, H. K.; Olsen, B. D. Adding the Effect of Topological Defects to the Flory−Rehner and Bray−Merrill Swelling Theories. *ACS Macro Lett.* **2021**, *10* (5), 531−537.
(8) Arora, A.; Lin, T.-S.; Beech, H. K.; Mochigase, H.; Wang, R.; Olsen, B. D. Fracture of Polymer Networks Containing Topological Defects. *Macromolecules* **2020**, *53* (17), 7346−7355.
(9) Danielsen, S. P. O.; Beech, H. K.; Wang, S.; El-Zaatari, B. M.; Wang, X.; Sapir, L.; Ouchi, T.; Wang, Z.; Johnson, P. N.; Hu, Y.; Lundberg, D. J.; Stoychev, G.; Craig, S. L.; Johnson, J. A.; Kalow, J. A.; Olsen, B. D.; Rubinstein, M. Molecular Characterization of Polymer Networks. *Chem. Rev.* **2021**, *121* (8), 5042−5092.
(10) de Gennes, P.-G. *Scaling Concepts in Polymer Physics*; Cornell University Press: Ithaca and London, 1979.
(11) Stauffer, D.; Coniglio, A.; Adam, M. Gelation and Critical Phenomena BT - Polymer Networks. *Adv. Polym. Sci.* **1982**, *44*, 103−158.
(12) Sakai, T.; Matsunaga, T.; Yamamoto, Y.; Ito, C.; Yoshida, R.; Suzuki, S.; Sasaki, N.; Shibayama, M.; Chung, U. Design and Fabrication of a High-Strength Hydrogel with Ideally Homogeneous Network Structure from Tetrahedron-like Macromonomers. *Macromolecules* **2008**, *41* (14), 5379−5384.
(13) Barney, C. W.; Ye, Z.; Sacligil, I.; McLeod, K. R.; Zhang, H.; Tew, G. N.; Riggleman, R. A.; Crosby, A. J. Fracture of Model End-Linked Networks. *Proc. Natl. Acad. Sci. U. S. A.* **2022**, *119* (7), 2−7.
(14) Cristiano, A.; Marcellan, A.; Long, R.; Hui, C.-Y.; Stolk, J.; Creton, C. An Experimental Investigation of Fracture by Cavitation of Model Elastomeric Networks. *J. Polym. Sci., Part B: Polym. Phys.* **2010**, *48* (13), 1409−1422.
(15) Cristiano, A.; Marcellan, A.; Keestra, B. J.; Steeman, P.; Creton, C. Fracture of Model Polyurethane Elastomeric Networks. *J. Polym. Sci., Part B: Polym. Phys.* **2011**, *49* (5), 355−367.
(16) Mark, J. E. Some Unusual Elastomers and Experiments on Rubberlike Elasticity. *Prog. Polym. Sci.* **2003**, *28* (8), 1205−1221.
(17) Yoo, S. H.; Yee, L.; Cohen, C. Effect of Network Structure on the Stress−Strain Behaviour of Endlinked PDMS Elastomers. *Polymer (Guildf).* **2010**, *51* (7), 1608−1613.
(18) Genesky, G. D.; Cohen, C. Toughness and Fracture Energy of PDMS Bimodal and Trimodal Networks with Widely Separated Precursor Molar Masses. *Polymer (Guildf).* **2010**, *51* (18), 4152−4159.
(19) Akagi, Y.; Sakurai, H.; Gong, J. P.; Chung, U.; Sakai, T. Fracture Energy of Polymer Gels with Controlled Network Structures. *J. Chem. Phys.* **2013**, *139* (14), 144905.
(20) Lin, S.; Zhao, X. Fracture of Polymer Networks with Diverse Topological Defects. *Phys. Rev. E* **2020**, *102* (5), No. 052503.
(21) Richbourg, N. R.; Peppas, N. A. The Swollen Polymer Network Hypothesis: Quantitative Models of Hydrogel Swelling, Stiffness, and Solute Transport. *Prog. Polym. Sci.* **2020**, *105*, No. 101243.
(22) Richbourg, N. R.; Wancura, M.; Gilchrist, A. E.; Toubbeh, S.; Harley, B. A. C.; Cosgriff-Hernandez, E.; Peppas, N. A. Precise Control of Synthetic Hydrogel Network Structure via Linear, Independent Synthesis-Swelling Relationships. *Sci. Adv.* **2021**, *7* (7), eabe3245.
(23) Flory, P. J.; Rehner, J. Statistical Mechanics of Cross-Linked Polymer Networks I. Rubberlike Elasticity. *J. Chem. Phys.* **1943**, *11* (11), 512−520.
(24) Flory, P. J.; Rehner, J. Statistical Mechanics of Cross-Linked Polymer Networks II. *Swelling. J. Chem. Phys.* **1943**, *11* (11), 521−526.
(25) Lake, G. J.; Thomas, A. G. The Strength of Highly Elastic Materials. *Proc. R. Soc. A Math. Phys. Eng. Sci.* **1967**, *300* (1460), 108−119.
(26) Anseth, K. S.; Bowman, C. N. Kinetic Gelation Model Predictions of Crosslinked Polymer Network Microstructure. *Chem. Eng. Sci.* **1994**, *49* (14), 2207−2217.
(27) Anseth, K. S.; Wang, C. M.; Bowman, C. N. Kinetic Evidence of Reaction Diffusion during the Polymerization of Multi(Meth)Acrylate Monomers. *Macromolecules* **1994**, *27* (3), 650−655.
(28) Anseth, K. S.; Anderson, K. J.; Bowman, C. N. Radical Concentrations, Environments, and Reactivities during Crosslinking Polymerizations. *Macromol. Chem. Phys.* **1996**, *197* (3), 833−848.
(29) Dušek, K. Phase Separation during the Formation of Three-dimensional Polymers. *J. Polym. Sci. Part C Polym. Symp.* **1967**, *16* (3), 1289−1299.
(30) Dušek, K.; Prins, W. Structure and Elasticity of Non-Crystalline Polymer Networks BT - Fortschritte Der Hochpolymeren-Forschung. In *Adv. Polym. Sci.*; Springer: Berlin, Heidelberg, 1969; Vol. *6*, pp 1−102. .
(31) Falender, J. R.; Yeh, G. S. Y.; Mark, J. E. The Effect of Chain Length Distribution on Elastomeric Properties. 1. Comparisons between Random and Highly Nonrandom Networks. *J. Am. Chem. Soc.* **1979**, *101* (24), 7353−7356.
(32) Pan, S.-J.; Mark, J. E. Model Networks of End-Linked Polydimethylsiloxane Chains. *Polym. Bull.* **1982**, *7* (11−12), 553−559.
(33) Viers, B. D.; Mark, J. E. Elastomeric Properties of Polysiloxane Networks. Bimodal Elastomers That Are Spatially Inhomogeneous and Others That Are Very Broadly Multimodal. *J. Macromol. Sci. Part A* **2007**, *44* (2), 131−138.
(34) Hirokawa, Y.; Jinnai, H.; Nishikawa, Y.; Okamoto, T.; Hashimoto, T. Direct Observation of Internal Structures in Poly(N -Isopropylacrylamide) Chemical Gels. *Macromolecules* **1999**, *32* (21), 7093−7099.
(35) Durmaz, S.; Okay, O. Phase Separation during the Formation of Poly(Acrylamide) Hydrogels. *Polymer (Guildf).* **2000**, *41* (15), 5729−5735.
(36) Aoki, H.; Tanaka, S.; Ito, S.; Yamamoto, M. Nanometric Inhomogeneity of Polymer Network Investigated by Scanning Near-Field Optical Microscopy. *Macromolecules* **2000**, *33* (26), 9650−9656.
(37) Madsen, F. B.; Daugaard, A. E.; Fleury, C.; Hvilsted, S.; Skov, A. L. Visualisation and Characterisation of Heterogeneous Bimodal PDMS Networks. *RSC Adv.* **2014**, *4* (14), 6939−6945.
(38) Dobson, A. L.; Huang, S.; Bowman, C. N. Modeling Phase Separation of Free-Radical Polymerizations in Crosslinked Networks. *Macromolecules* **2024**, *57* (3), 894−902.
(39) Corrigan, N.; Jung, K.; Moad, G.; Hawker, C. J.; Matyjaszewski, K.; Boyer, C. Reversible-Deactivation Radical Polymerization (Controlled/Living Radical Polymerization): From Discovery to Materials Design and Applications. *Prog. Polym. Sci.* **2020**, *111*, No. 101311.
(40) Ide, N.; Fukuda, T. Nitroxide-Controlled Free-Radical Copolymerization of Vinyl and Divinyl Monomers. Evaluation of Pendant-Vinyl Reactivity. *Macromolecules* **1997**, *30* (15), 4268−4271.

https://doi.org/10.1021/acs.macromol.4c00905
Macromolecules 2024, 57, 8698−8711

(41) Ide, N.; Fukuda, T. Nitroxide-Controlled Free-Radical Copolymerization of Vinyl and Divinyl Monomers. 2. Gelation. *Macromolecules* **1999**, *32* (1), 95−99.
(42) Bannister, I.; Billingham, N. C.; Armes, S. P.; Rannard, S. P.; Findlay, P. Development of Branching in Living Radical Copolymerization of Vinyl and Divinyl Monomers. *Macromolecules* **2006**, *39* (22), 7483−7492.
(43) Vo, C.-D.; Rosselgong, J.; Armes, S. P.; Billingham, N. C. RAFT Synthesis of Branched Acrylic Copolymers. *Macromolecules* **2007**, *40* (20), 7119−7125.
(44) Roos, S. G.; Müller, A. H. E.; Matyjaszewski, K. Copolymerization of n -Butyl Acrylate with Methyl Methacrylate and PMMA Macromonomers: Comparison of Reactivity Ratios in Conventional and Atom Transfer Radical Copolymerization. *Macromolecules* **1999**, *32* (25), 8331−8335.
(45) Gao, H.; Li, W.; Matyjaszewski, K. Synthesis of Polyacrylate Networks by ATRP: Parameters Influencing Experimental Gel Points. *Macromolecules* **2008**, *41* (7), 2335−2340.
(46) Gao, H.; Miasnikova, A.; Matyjaszewski, K. Effect of Cross-Linker Reactivity on Experimental Gel Points during ATRcP of Monomer and Cross-Linker. *Macromolecules* **2008**, *41* (21), 7843−7849.
(47) Gao, H.; Matyjaszewski, K. Synthesis of Functional Polymers with Controlled Architecture by CRP of Monomers in the Presence of Cross-Linkers: From Stars to Gels. *Prog. Polym. Sci.* **2009**, *34* (4), 317−350.
(48) Cuthbert, J.; Balazs, A. C.; Kowalewski, T.; Matyjaszewski, K. STEM Gels by Controlled Radical Polymerization. *Trends Chem.* **2020**, *2* (4), 341−353.
(49) Cuthbert, J.; Wanasinghe, S. V.; Matyjaszewski, K.; Konkolewicz, D. Are RAFT and ATRP Universally Interchangeable Polymerization Methods in Network Formation? *Macromolecules* **2021**, *54* (18), 8331−8340.
(50) Ducrot, E.; Chen, Y.; Bulters, M.; Sijbesma, R. P.; Creton, C. Toughening Elastomers with Sacrificial Bonds and Watching Them Break. *Science (80-.)* **2014**, *344* (6180), 186−189.
(51) Ducrot, E.; Montes, H.; Creton, C. Structure of Tough Multiple Network Elastomers by Small Angle Neutron Scattering. *Macromolecules* **2015**, *48* (21), 7945−7952.
(52) Ducrot, E.; Creton, C. Characterizing Large Strain Elasticity of Brittle Elastomeric Networks by Embedding Them in a Soft Extensible Matrix. *Adv. Funct. Mater.* **2016**, *26* (15), 2482−2492.
(53) Bekanova, M. Z.; Neumolotov, N. K.; Jablanović, A. D.; Plutalova, A. V.; Chernikova, E. V.; Kudryavtsev, Y. V. Thermal Stability of RAFT-Based Poly(Methyl Methacrylate): A Kinetic Study of the Dithiobenzoate and Trithiocarbonate End-Group Effect. *Polym. Degrad. Stab.* **2019**, *164*, 18−27.
(54) Li, M.; De, P.; Gondi, S. R.; Sumerlin, B. S. End Group Transformations of RAFT-generated Polymers with Bismaleimides: Functional Telechelics and Modular Block Copolymers. *J. Polym. Sci. Part A Polym. Chem.* **2008**, *46* (15), 5093−5100.
(55) Coessens, V.; Pintauer, T.; Matyjaszewski, K. Functional Polymers by Atom Transfer Radical Polymerization. *Prog. Polym. Sci.* **2001**, *26* (3), 337−377.
(56) Millereau, P.; Ducrot, E.; Clough, J. M.; Wiseman, M. E.; Brown, H. R.; Sijbesma, R. P.; Creton, C. Mechanics of Elastomeric Molecular Composites. *Proc. Natl. Acad. Sci. U. S. A.* **2018**, *115* (37), 9110−9115.
(57) He, X.; Tang, J. Kinetics of Self-condensing Vinyl Hyperbranched Polymerization in Three-dimensional Space. *J. Polym. Sci. Part A Polym. Chem.* **2008**, *46* (13), 4486−4494.
(58) Wang, L.; He, X. Investigation of AB n (n = 2, 4) Type Hyperbranched Polymerization with Cyclization and Steric Factors: Influences of Monomer Concentration, Reactivity, and Substitution Effect. *J. Polym. Sci. Part A Polym. Chem.* **2009**, *47* (2), 523−533.
(59) Furuya, T.; Koga, T. Molecular Simulation of Polymer Gels Synthesized by Free Radical Copolymerization: Effects of Concentrations and Reaction Rates on Structure and Mechanical Properties. *Polymer (Guildf).* **2023**, *279* (March), No. 126012.
(60) Furuya, T.; Koga, T. Comparison of Gels Synthesized by Controlled Radical Copolymerization and Free Radical Copolymerization: Molecular Dynamics Simulation. *Soft Matter* **2024**, *20* (6), 1164−1172.
(61) Lyu, J.; Gao, Y.; Zhang, Z.; Greiser, U.; Polanowski, P.; Jeszka, J. K.; Matyjaszewski, K.; Tai, H.; Wang, W. Monte Carlo Simulations of Atom Transfer Radical (Homo)Polymerization of Divinyl Monomers: Applicability of Flory−Stockmayer Theory. *Macromolecules* **2018**, *51* (17), 6673−6681.
(62) Lyu, J.; Gao, Y.; Zhang, Z.; Greiser, U.; Tai, H.; Wang, W. Can Flory-Stockmayer Theory Be Applied to Predict Conventional Free Radical Polymerization of Multivinyl Monomers? A Study via Monte Carlo Simulations. *Sci. China Chem.* **2018**, *61* (3), 319−327.
(63) Gao, H.; Polanowski, P.; Matyjaszewski, K. Gelation in Living Copolymerization of Monomer and Divinyl Cross-Linker: Comparison of ATRP Experiments with Monte Carlo Simulations. *Macromolecules* **2009**, *42* (16), 5925−5932.
(64) Perrier, S. 50th Anniversary Perspective: RAFT Polymerization—A User Guide. *Macromolecules* **2017**, *50* (19), 7433−7447.
(65) Matyjaszewski, K. Atom Transfer Radical Polymerization (ATRP): Current Status and Future Perspectives. *Macromolecules* **2012**, *45* (10), 4015−4039.
(66) Vana, P. Kinetic Aspects of RAFT Polymerization. *Macromol. Symp.* **2007**, *248* (1), 71−81.
(67) Konkolewicz, D.; Hawkett, B. S.; Gray-Weale, A.; Perrier, S. RAFT Polymerization Kinetics: Combination of Apparently Conflicting Models. *Macromolecules* **2008**, *41* (17), 6400−6412.
(68) Konkolewicz, D.; Hawkett, B. S.; Gray-Weale, A.; Perrier, S. RAFT Polymerization Kinetics: How Long Are the Cross-terminating Oligomers? *J. Polym. Sci. Part A Polym. Chem.* **2009**, *47* (14), 3455−3466.
(69) Ting, S. R. S.; Davis, T. P.; Zetterlund, P. B. Retardation in RAFT Polymerization: Does Cross-Termination Occur with Short Radicals Only? *Macromolecules* **2011**, *44* (11), 4187−4193.
(70) Bradford, K. G. E.; Petit, L. M.; Whitfield, R.; Anastasaki, A.; Barner-Kowollik, C.; Konkolewicz, D. Ubiquitous Nature of Rate Retardation in Reversible Addition-Fragmentation Chain Transfer Polymerization. *J. Am. Chem. Soc.* **2021**, *143* (42), 17769−17777.
(71) Truong, N. P.; Jones, G. R.; Bradford, K. G. E.; Konkolewicz, D.; Anastasaki, A. A Comparison of RAFT and ATRP Methods for Controlled Radical Polymerization. *Nat. Rev. Chem.* **2021**, *5* (12), 859−869.
(72) Yu, Q.; Zeng, F.; Zhu, S. Atom Transfer Radical Polymerization of Poly(Ethylene Glycol) Dimethacrylate. *Macromolecules* **2001**, *34* (6), 1612−1618.
(73) Yu, Q.; Xu, S.; Zhang, H.; Ding, Y.; Zhu, S. Comparison of Reaction Kinetics and Gelation Behaviors in Atom Transfer, Reversible Addition−Fragmentation Chain Transfer and Conventional Free Radical Copolymerization of Oligo(Ethylene Glycol) Methyl Ether Methacrylate and Oligo(Ethylene Glycol) Dimetha. *Polymer (Guildf).* **2009**, *50* (15), 3488−3494.
(74) Gao, H.; Min, K.; Matyjaszewski, K. Determination of Gel Point during Atom Transfer Radical Copolymerization with Cross-Linker. *Macromolecules* **2007**, *40* (22), 7763−7770.
(75) Lin, F.-Y.; Yan, M.; Cochran, E. W. Gelation Suppression in RAFT Polymerization. *Macromolecules* **2019**, *52* (18), 7005−7015.
(76) Moad, G. RAFT (Reversible Addition-Fragmentation Chain Transfer) Crosslinking (Co)Polymerization of Multi-Olefinic Monomers to Form Polymer Networks. *Polym. Int.* **2015**, *64* (1), 15−24.
(77) Gong, J. P.; Katsuyama, Y.; Kurokawa, T.; Osada, Y. Double-Network Hydrogels with Extremely High Mechanical Strength. *Adv. Mater.* **2003**, *15* (14), 1155−1158.
(78) Brown, H. R. A Model of the Fracture of Double Network Gels. *Macromolecules* **2007**, *40* (10), 3815−3818.
(79) Slootman, J.; Yeh, C. J.; Millereau, P.; Comtet, J.; Creton, C. A Molecular Interpretation of the Toughness of Multiple Network Elastomers at High Temperature. *Proc. Natl. Acad. Sci. U. S. A.* **2022**, *119* (13), 1−11.

https://doi.org/10.1021/acs.macromol.4c00905
Macromolecules 2024, 57, 8698−8711

(80) Creton, C. 50th Anniversary Perspective: Networks and Gels: Soft but Dynamic and Tough. *Macromolecules* **2017**, *50* (21), 8297−8316.
(81) Ishikawa, S.; Iwanaga, Y.; Uneyama, T.; Li, X.; Hojo, H.; Fujinaga, I.; Katashima, T.; Saito, T.; Okada, Y.; Chung, U.; Sakumichi, N.; Sakai, T. Percolation-Induced Gel−Gel Phase Separation in a Dilute Polymer Network. *Nat. Mater.* **2023**, *22* (12), 1564−1570.
(82) Bagheri, A.; Fellows, C. M.; Boyer, C. Reversible Deactivation Radical Polymerization: From Polymer Network Synthesis to 3D Printing. *Adv. Sci.* **2021**, *8* (5), No. 2003701.

https://doi.org/10.1021/acs.macromol.4c00905
Macromolecules 2024, 57, 8698−8711